

**UREA AND URIC ACID ADSORPTION
BY NANOPOROUS BIOMATERIALS**

by

CHEAH WEE KEAT

Thesis submitted in fulfilment of the requirements

for the degree of

Doctor of Philosophy

May 2016

DEDICATION

I would like to dedicate this thesis to

my wonderful family...

my father,

my mother,

my sisters

and my grandparents who almost got to see me graduate.

ACKNOWLEDGEMENT

I would like to extend a word of acknowledgment and express my heartfelt gratitude to the individuals who have helped me throughout the duration of my PhD project. Without them, I doubt that I could have completed my PhD successfully.

First and foremost, my heartfelt appreciation to the School of Materials and Mineral Resources Engineering, Universiti Sains Malaysia, the respectful dean Professor Zuhailawati Hussain, all the technical and administrative staff, for providing professional assistance and facilities.

I would like to express my appreciation to Dr. Yeoh Fei Yee, as both my supervisor and mentor, for his guidance and encouragement during my research and writing of this thesis. His support guided me to overcome most obstacles faced during this project, without which I could not have progress as smoothly. I would like to thank my co-supervisor, Professor Radzali Othman, for his support throughout this project. Special thanks goes to Dr. Sim Yoke Leng (Department of Chemical Science, Universiti Tunku Abdul Rahman) for her invaluable chemistry input.

I would like to acknowledge the Ministry of Education Malaysia, for providing me not only the financial support through the MyBrain15 scholarship program, but also the necessary fundings for this research through the Fundamental Research Grant Scheme (FRGS) and Exploratory Research Grant Scheme (ERGS).

Also, I would like to thank my friends and fellow postgraduates. Special mention to my fellow Advanced Nanoporous Materials Group labmates. To my lunchmates, thank you for the countless technical and non-tech discussion sessions.

CHEAH WEE KEAT

May 2016

TABLE OF CONTENTS

ACKNOWLEDGEMENT	ii
TABLE OF CONTENTS	iii
LIST OF TABLES	vii
LIST OF FIGURES	viii
LIST OF ABBREVIATIONS	xi
LIST OF SYMBOLS	xiii
ABSTRAK	xiv
ABSTRACT	xvi
CHAPTER 1: INTRODUCTION	1
1.1 Research Background.....	1
1.2 Problem Statement	4
1.3 Research Objectives	6
1.4 Scope of Research	7
1.5 Thesis Outline.....	7
CHAPTER 2: LITERATURE REVIEW	10
2.1 Human Kidney and Kidney Diseases	10
2.2 Uremic Toxins and Classification	12
2.2.1 Urea.....	13
2.2.2 Uric Acid.....	15
2.2.3 Beer-Lambert Law	16
2.3 Nanoporous Biomaterials for Uremic Toxin Adsorption in an Artificial Kidney System	17
2.3.1 Artificial Kidney Systems	21
2.3.1(a) Hemoperfusion.....	21
2.3.1(b) Hemodialysis and Miniaturised Hemodialysis Systems.....	23

2.3.1(c)	Hemodialysis Based Wearable Artificial Kidney Prototypes.....	24
2.3.1(d)	Peritoneal Dialysis	24
2.3.2	Nanoporous Adsorbents for Hemoperfusion	26
2.3.3	Nanoporous Adsorbents in a Miniaturised Hemodialysis System.....	31
2.4	Emerging Nanoporous Biomaterials	34
2.4.1	Activated Carbon	35
2.4.1(a)	Activated Carbon Fibre Derived from Empty Fruit Bunch Fibre.	37
2.4.2	Mesoporous Silica.....	39
2.4.2(a)	Amine Functionalised Mesoporous Silica	42
2.4.3	Mesoporous Hydroxyapatite	43
2.5	Adsorption	45
2.5.1	Adsorption Isotherm	47
CHAPTER 3: METHODOLOGY.....		49
3.1	Introduction	49
3.2	Synthesis of Hollow Activated Carbon Fibre Derived from Palm Oil Empty Fruit Bunch Fibre	51
3.2.1	Empty Fruit Bunch Fibre	51
3.2.2	Acid Treatment.....	52
3.2.3	Carbonisation and Activation.....	53
3.3	Synthesis of Mesoporous Silica SBA-15	53
3.3.1	Chemicals.....	53
3.3.2	Method	54
3.3.2	Synthesis of Amine Functionalised Mesoporous Silica SBA-15.....	55
3.4	Synthesis of Mesoporous Hydroxyapatite.....	56
3.4.1	Chemicals.....	56
3.4.2	Method	57
3.5	Characterisation of Nanoporous Biomaterials.....	59

3.5.1	Scanning Electron Microscopy and Energy Dispersive X-Ray Spectroscopy	59
3.5.2	X-Ray Diffraction Analysis	59
3.5.3	Thermogravimetric Analysis.....	60
3.5.4	Fourier Transform Infrared Spectroscopy.....	60
3.5.5	Transmission Electron Microscopy	61
3.5.6	Nitrogen Adsorption Analysis.....	61
3.6	Uremic Toxin Adsorption Test.....	62
3.6.1	Urea and Uric Acid Calibration Curve.....	62
3.6.2	Urea Adsorption by Nanoporous Biomaterials	65
3.6.3	Urea Adsorption Kinetics by Activated Carbon Fibre	66
3.6.4	Urea Adsorption Kinetics by Mesoporous Silica.....	67
3.6.5	Uric Acid Adsorption Kinetics by Mesoporous Silica.....	67
CHAPTER 4: RESULTS AND DISCUSSION		69
4.1	Introduction	69
4.2	Synthesis and Characterisation of Nanoporous Biomaterials	69
4.2.1	Synthesis and Characterisation of Activated Carbon Fibre	70
4.2.1(a)	Morphological Analysis.....	71
4.2.1(b)	Phase Analysis	75
4.2.1(c)	Pore Characterisation of Activated Carbon Fibre.....	77
4.2.2	Synthesis and Characterisation of Mesoporous Silica and Amine functionalised Mesoporous Silica.....	80
4.2.2.1	Phase Identification.....	80
4.2.2.2	Elimination of Surfactant.....	82
4.2.2.3	Surface Functionalisation of Mesoporous Silica	85
4.2.2.4	Pore Characterisation of Mesoporous Silica.....	87
4.2.3	Synthesis and Characterisation of Mesoporous Hydroxyapatite	92
4.2.3(a)	Phase Identification.....	92

4.2.3(b)	Elimination of Surfactant.....	94
4.2.3(c)	Pore Characterisation of Mesoporous Hydroxyapatite.....	96
4.3	Urea Adsorption by Nanoporous Biomaterials	100
4.3.1	Evaluation of Urea Adsorption Capacity	100
4.3.2	Urea Adsorption Kinetics by Activated Carbon Fibre.....	104
4.3.3	Urea Adsorption Kinetics by Mesoporous Silica.....	108
4.4	Uric Acid Adsorption Kinetics by Mesoporous Silica.....	114
CHAPTER 5: SUMMARY AND CONCLUSION.....		122
5.1	Conclusion.....	122
5.2	Summary	124
5.3	Recommendations for Future Work	124
REFERENCES.....		126
APPENDIX A		
APPENDIX B		
APPENDIX C		
APPENDIX D		
APPENDIX E		
APPENDIX F		
APPENDIX G		

LIST OF TABLES

Table 1.1: Hemodialysis and ideal artificial kidney.....	4
Table 2.1: Normal concentration, uremic concentration and physical properties of urea.....	14
Table 2.2: Normal concentration, uremic concentration and physical properties of uric acid.....	15
Table 2.3: Highlighted nanoporous materials in artificial kidney systems.....	20
Table 2.4: Review studies of SBA-15 synthesis parameters and resultant pore size, BET surface area and pore volume	40
Table 3.1: Acids used, corresponding manufacturer and sample denotation.....	52
Table 3.2: Chemicals used for the synthesis of mesoporous silica SBA-15.....	54
Table 3.3: Chemicals used for synthesis of amine functionalised MS	56
Table 3.4: Chemicals used for the synthesis of mesoporous HAp.....	57
Table 4.1: Surface area, pore volume and pore diameter of MS-B, MS-S, MS-N and MS-DN.....	89
Table 4.2: Crystallite size calculated from (002) peak	94
Table 4.3: Matrix of samples for urea adsorption capacity test categorised by the nanoporous biomaterial group and respective urea adsorption capacity	101
Table 4.4: BET surface area, nominal rate constant (k), urea apparent adsorption capacity (A) and normalised surface area adsorption capacity (M/a) of CAC and ACF.....	106
Table 4.5: BET surface area, nominal rate constant (k), apparent urea adsorption capacity (A) and normalised surface area adsorption capacity (M/a) of C, S, N and AC	109
Table 4.6: BET surface area, nominal rate constant of adsorption (k1), uric acid adsorption capacity (A1), nominal rate constant of desorption (k2), desorption capacity (A2) and equilibrium adsorption (A) for MS and SG.....	118

LIST OF FIGURES

Figure 1.1: Uremic toxin retention cycle pre- and during hemodialysis.....	2
Figure 1.2: Project outline.....	8
Figure 2.1: Schematic diagram of kidney and a nephron. Major components: Co = cortex, Me = medulla, Pe = pelvis. Nephron: G = glomerulus, B = Bowman's capsule, P = proximal tubule, H = loop of Henle, D = distal tubule, and C = collecting duct (Dankers et al., 2011)	10
Figure 2.2: ESRD treatment modality (Health and Services, 2011)	12
Figure 2.3: Chemical structure of urea (Wernert et al., 2005)	15
Figure 2.4: Chemical structure of uric acid molecule (Wernert et al., 2005)	16
Figure 2.5: Location of nanoporous adsorbent utilised in (a) hemoperfusion and (b) hemodialysis.....	19
Figure 2.6: Schematic diagram of a typical hemoperfusion system	22
Figure 2.7: Schematic diagram of a typical hemodialysis system	22
Figure 2.8: Wearable artificial kidney (Gura et al., 2008).....	24
Figure 2.9: Peritoneal dialysis.....	25
Figure 2.10: Internal and external surface functionalisation (mesoporous silica)	31
Figure 2.11: Classification of nanoporous materials: (i) IUPAC classification and (ii) ISO nanoporous classification.....	35
Figure 2.12: Synthesis of mesoporous silica from micelle template [adapted from (Vinu et al., 2006)]	41
Figure 2.13: Schematic diagram of a surface phenomenon in adsorption process	45
Figure 2.14: Types of adsorption isotherms (Weidenthaler, 2011)	47
Figure 3.1: Research methodology outline	49
Figure 3.2: Flowchart for synthesis of ACF derived from palm oil EFB	51
Figure 3.3: Cleaned EFB fibre	52
Figure 3.4: Flowchart for synthesis of mesoporous silica SBA-15	54
Figure 3.5: Flowchart for post grafting of mesoporous silica SBA-15 with amine and diamine functional group	55
Figure 3.6: Flowchart for synthesis of mesoporous hydroxyapatite	57
Figure 3.7: Linear calibration curve of urea solution at wavelength 200nm	63
Figure 3.8: Linear calibration curve of uric acid solution at wavelength 286 nm	64

Figure 4.1: SEM micrographs of (a) IACF-S, (b) IACF-N, (c) IACF-P, (d) OACF-A, (e) OACF-C and (f) raw EFB fibre, at the edge of the fibre and along the length of the fibre	72
Figure 4.2: Diffusion path length, d of (a) ACF and (b) PAC	73
Figure 4.3: (a) Silica particle detached from IACF-D and (b) EDX of silica particle	75
Figure 4.4: XRD patterns for IACF-P, OACF-C and commercial activated carbon (CAC).....	77
Figure 4.5: Nitrogen adsorption isotherms of CAC and ACF samples	78
Figure 4.6: DFT pore size distribution of IACF-P.....	79
Figure 4.7: BET surface area and pore volume of various ACF samples and commercial AC	80
Figure 4.8: XRD pattern of MS-B (before calcination) and MS-S (SBA-15 after calcination).....	81
Figure 4.9: XRD pattern of sample MS-S (pure SBA-15), MS-N (APTES functionalised silica) and MS-DN (AEAPTS functionalised silica).....	82
Figure 4.10: Burn off profile for MS-B	83
Figure 4.11: FTIR spectra of MS-B and MS-S	84
Figure 4.12: FTIR spectra of MS-S, MS-N and MS-DN.....	86
Figure 4.13: Chemical structure of APTES and AEAPTS (Maria Chong and Zhao, 2003; Grau et al., 2015).....	87
Figure 4.14: Nitrogen adsorption isotherm of MS-B, MS-S, MS-N and MS-DN.....	88
Figure 4.15: Reduction in pore diameter due to grafting process	89
Figure 4.16: TEM micrograph of (a) MS-S (b) MS-N and (c) MS-DN	91
Figure 4.17: XRD patterns of HAp precipitates before and after calcination.....	93
Figure 4.18: FTIR spectra of HAP-B (before calcination) and HAP-C (after calcination).....	94
Figure 4.19: TEM micrographs of HAP-C and HAF-C from axial and parallel view, with circled region indicating observed mesopores	96
Figure 4.20: Schematics of HAp cylindrical pores as observed from different direction with varying view structure of pores (a) axial view and (b) parallel view .	97
Figure 4.21: Nitrogen adsorption-desorption isotherm of HAP and HAF.....	98
Figure 4.22: BJH desorption pore size distribution of samples HAP and HAF	99
Figure 4.23: Surface area and adsorption capacity of nanoporous biomaterials and commercial samples	101

Figure 4.24: Normalised surface area adsorption capacity (M/a) for HAp samples	103
Figure 4.25: Normalised surface area adsorption capacity (M/a) for ACF and MS	104
Figure 4.26: Urea adsorption kinetics by CAC and ACF	105
Figure 4.27: FTIR spectra of ACF samples	107
Figure 4.28: MS and CAC urea adsorption kinetics	108
Figure 4.29: Proposed adsorption mechanism of urea on (a) MS-S and (b) MS-N.	111
Figure 4.30: FTIR spectrum of MS-S before and after urea adsorption	113
Figure 4.31: FTIR spectrum of MS-N before and after urea adsorption	114
Figure 4.32: Obtained uric acid adsorption data points (a) MS-N and (b) MS-DN.	115
Figure 4.33: Typical adsorption curve of uric acid by mesoporous silica	115
Figure 4.34: (a) Adsorption and desorption curves, (b) resulting sum of adsorption and desorption curves.....	116
Figure 4.35: MS-S, MS-N, MS-DN and SG uric acid adsorption kinetics.....	117
Figure 4.36: FTIR spectra of MS-S before and after uric acid adsorption	119
Figure 4.37: FTIR spectra of MS-DN before and after uric acid adsorption.....	119
Figure 4.38: FTIR spectra of MS-N before and after uric acid adsorption.....	120
Figure 4.39: Proposed mechanism for uric acid adsorption by (a) MS-S, (b) MS-N and (c) MS-DN.....	121

LIST OF ABBREVIATIONS

AC	: Activated carbon
ACF	: Activated carbon fibre
AEAPTS	: N-(2-aminoethyl)-3-aminopropyltrimethoxysilane
APTES	: (3-Aminopropyl)triethoxysilane
ARF	: Acute renal failure
BET	: Brunauer–Emmett–Teller
BJH	: Barrett-Joyner-Halenda
Ca ⁺	: Calcium ion
CAC	: Commercial activated carbon
CKD	: Chronic kidney disease
C _{MAX}	: Maximum uremic concentration
C _N	: Normal / healthy uremic concentration
CTAB	: Cetrimonium bromide
C _U	: Uremic concentration, concentration of ESRD patients
DI	: Deionised
DFT	: Density Functional Theory
EDX	: Energy dispersive x-ray spectroscopy
EFB	: Empty fruit bunch
ESAO	: European Society of Artificial Organs
ESRD	: End stage renal disease
EUTox	: European Uremic Toxin Workgroup
FESEM	: Field emission scanning electron microscope
FSM-16	: Folded Sheets Mesoporous Materials No. 16

FTIR	: Fourier transform infrared
GAC	: Granular activated carbon
HAp	: Hydroxyapatite
HCl	: Hydrochloric acid
HD	: Hemodialysis
HP	: Hemoperfusion
HRTEM	: High resolution transmission electron microscope
IUPAC	: International Union of Pure and Applied Chemistry
KBr	: Potassium bromide
MCM-41	: Mobil Composition of Matter No. 41
MS	: Mesoporous silica
N ₂	: Nitrogen gas
PAC	: Powdered activated carbon
PO ₄ ³⁻	: Phosphate ion
RRT	: Renal replacement therapy
SBA-15	: Santa Barbara-15
TEM	: Transmission electron microscopy
TEOS	: Tetraethyl orthosilicate
TGA	: Thermogravimetric analysis
TMOS	: Tetramethyl orthosilicate
TPOS	: Tetrapropyl orthosilicate
WAK	: Wearable artificial kidney
XRD	: X-ray diffraction

LIST OF SYMBOLS

C	: concentration (mol/L)
C_i	: initial concentration (mg/L)
C_f	: final concentration (mg/L)
m	: mass (g)
M	: molarity (mol/L),
MW	: molecular weight (g/mol).
Q	: amount of adsorbed (mg/g)
V	: volume of the solution (L)
y	: adsorbed at time (t)
A	: apparent adsorption capacity (mg/g)
k	: nominal rate constant (mg/g/s)
M/a	: normalised surface area adsorption capacity (molecules/nm ²)
A1	: adsorption capacity (mg/g)
k1	: nominal rate constant of adsorption (mg/g/s)
A2	: desorption capacity (mg/g)
k2	: nominal rate constant of desorption (mg/g/s)

PENJERAPAN UREA DAN ASID URIK OLEH BAHAN BIO BERLIANG NANO

ABSTRAK

Kelemahan hemodialisis zaman ini telah menjadi punca penyelidikan dan pembangunan beberapa prototaip ginjal buatan mudah alih. Komponen utama model mudah alih ini (berbanding hemodialisis) ialah sistem dialisat tertutup. Secara tipikalnya, model-model ini biasanya menggunakan karbon teraktif sebagai bahan penjerap. Penggunaan bahan penjerap yang lebih unggul, jumlah dialisat yang diperlukan untuk penyingkiran toksin uremik boleh dikurangkan dan dikitar semula. Motivasi utama bagi penyelidikan ini ialah kekurangan pemilihan bahan untuk bahan penjerap dalam model-model ini. Oleh itu, objektif projek ini ialah sintesis dan penilaian tiga jenis biobahan berliang nano yang baru, iaitu gentian karbon teraktif berongga (ACF), silika berliang meso (MS) dan hidroksiapatit berliang meso, dengan sasaran untuk penyingkiran konstituen utama toksin uremik, iaitu urea dan asid urik. ACF telah diperolehi melalui kaedah pengaktifan asid dengan menggunakan asid-asid yang berbeza; asid bukan organik sulfurik, nitrik dan fosforik; asid organik asetik dan sitrik. MS dan HAp telah disintesis melalui kaedah templat lembut dengan surfaktan Pluronic. Keputusan awal penjerapan urea telah menunjukkan bahawa MS dengan kumpulan berfungsi amina dan ACF terawat asid sulfuric adalah sangat baik (550 mg/g) berbanding dengan karbon teraktif komersil (CAC). Ujian kinetik penjerapan urea telah mendedahkan mekanisma penjerapan urea oleh ACF (jerapan fizikal) dan MS (jerapan kimia). MS amina dan diamina menjerap lebih daripada 30 molekul per nm² (jerapan kimia yang kuat) berbanding MS biasa, CAC dan pelbagai

ACF, yang telah menjerap kurang daripada 10 molekul per nm^2 (jerapan fizikal). Faktor-faktor utama yang mempengaruhi kapasiti jerapan ialah keliangan dan kimia permukaan yang sesuai, yang mana kedua-duanya dipunyai oleh MS amina dan diamina. Kebolehubahan permukaan berfungsi bagi MS merupakan asas untuk ujian jerapan urik asid seterusnya. Satu hipotesis peningkatan jerapan asid urik oleh MS berfungsi amina merupakan melalui tindak balas kimia asid-amina. Jerapan asid urik oleh MS tidak mengikut keluk jerapan teori. Analisa yang mendalam dengan menggunakan aplikasi MATLAB menunjukkan bahawa MS telah menjalani jerapan dan nyahrepan serentak, dengan kadar jerapan permulaan setinggi 20.3 mg/g/s berbanding gel silica dengan kadar jerapan hanya 0.39 mg/g/s. Sebagai kesimpulan, secara keseluruhannya, keputusan jerapan urea dan asid urik MS dan ACF lebih baik berbanding CAC dan gel silica komersil.

UREA AND URIC ACID ADSORPTION BY NANOPOROUS BIOMATERIALS

ABSTRACT

The limitations of the present hemodialysis have led towards the research and development of several wearable artificial kidney prototypes. The most important component of the miniaturised model is the closed-system dialysate, achieved through the utilisation of solid activated carbon as adsorbents. With the application of superior alternative adsorbents, the amount of dialysate required could be reduced due to efficient regeneration. The main motivation for this project is the lack of adsorbent materials selection. Thus, this project aims to synthesise and evaluate three emerging nanoporous biomaterials, i.e. hollow activated carbon fibre (ACF), mesoporous silica (MS) and mesoporous hydroxyapatite (HAp), targeting major uremic toxin constituent urea and uric acid. ACF was obtained through the acid activation route, with variation in acid used; inorganic acids sulphuric, nitric and phosphoric; organic acids acetic and citric. MS and HAp was synthesised through soft templating route using Pluronics surfactant. Results show that amine functionalised MS and sulphuric acid treated ACF performed well in the preliminary urea adsorption capacity evaluation (550 mg/g), as compared to the control commercial activated carbon (CAC) (350 mg/g). Subsequent urea kinetics study revealed better understanding of urea adsorption mechanism by ACF and MS, whereby ACF and MS operate through physisorption and chemisorption respectively. Amine and diamine MS adsorbed more than 30 molecules per nm² (strong chemisorption interaction) compared to bare MS, CAC and various ACF, which adsorbed less than 10 molecules per nm² (physisorption). The most important factors which govern adsorption capacity are porosity and suitable surface chemistry,

both which are possessed by amine and diamine MS. The flexibility of surface functionalisation of MS is the basis of subsequent uric acid adsorption kinetics test. Amine functionalised MS is hypothesised to improve uric acid adsorption through acid-amine reaction. Uric acid adsorption by MS did not follow theoretical adsorption curve. Further analysis using MATLAB curve fit revealed that MS underwent simultaneous adsorption-desorption, with initial adsorption rates as high as 20.3 mg/g/s compared to commercial silica gel, with initial adsorption rate of 0.39 mg/g/s. As a conclusion, on a whole, MS and ACF performed better than the benchmarked CAC and commercial silica gel in terms of urea and uric acid adsorption.

CHAPTER 1: INTRODUCTION

1.1 Research Background

Currently, the commonly accepted treatment for patients' who suffer from kidney failure is hemodialysis. Nevertheless, due to the size of hemodialysis machines, patients would have to endure mobility restraint. Kidney transplant is by far the most ideal renal replacement treatment option but the number of patients usually greatly outnumbers the donors. The limited supply of available kidneys is the main reason kidney transplants are close to impossible, not to mention the donor-patient compatibility of the organ which reduces the chance for a patient to accept the treatment. Peritoneal dialysis is a smaller renal replacement setup using the patient's peritoneum in the abdomen as a membrane for dialysis, which offers better mobility and flexibility for uremic toxin removal. However, the patients are faced with risks for future complications, such as infection in the peritoneum. Patients undergoing peritoneal dialysis have better mobility as compared to hemodialysis (Diaz-Buxo et al., 1981; Olcott IV et al., 1983; Kooman et al., 2015). Though peritoneal dialysis shows better survival rates during initial stages of dialysis, the survival rates drop significantly over a longer treatment period compared to hemodialysis. Complications such as infection or peritonitis ultimately highlight hemodialysis as a better option (Sinnakirouchenan and Holley, 2011). Thus, despite all the disadvantages, hemodialysis still remains the most feasible option in terms of safety, cost and treatment efficiency.

The current hemodialysis setup which uses diffusion-based membrane technology is not efficient since uremic toxins with high molecular mass could not be removed (Vanholder et al., 2003). The residual uremic toxins which were not

removed would gradually build up in the patients' body. The retention of uremic toxin similar to a slow and gradual poisoning (uremia). Eventually, life span is shortened as the suffering period is prolonged. Each individual uremic toxin build-up in a chronic kidney disease (CKD) patient would cause its own complications. For instance, uric acid retention would cause serious problems such as gout, diabetes and leukemia (Kang, 2014). Present hemodialysis is not a perfect solution; the period of initial uremic toxin poisoning leading up until the upper concentration threshold which the human body could withstand, is merely prolonged. One other inherent problem of hemodialysis is that it is not a continuous uremic toxin removal process. High and low uremic toxin cyclic levels during treatment and non-treatment periods would cause a state of shock on a patient's body (Figure 1.1).

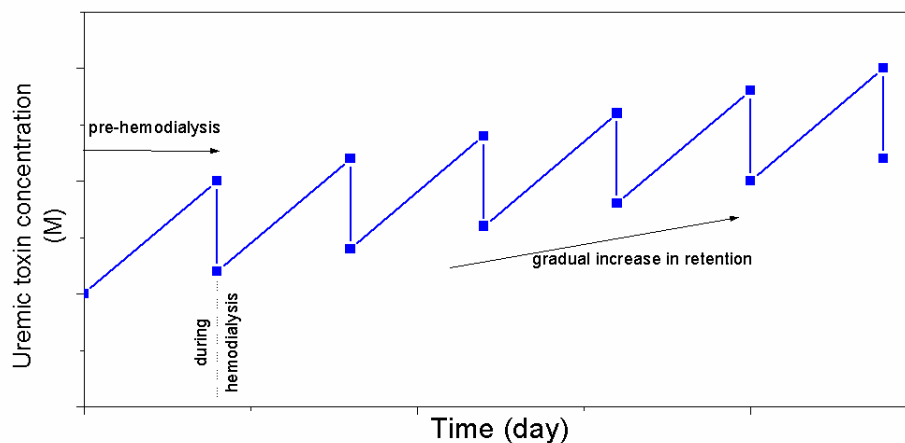


Figure 1.1: Uremic toxin retention cycle pre- and during hemodialysis

Furthermore, the mobility of patients is hindered due to their dependency on hemodialysis. Patients would have to travel to hemodialysis centres for treatment on alternate days during a week (3 times), and undergo hemodialysis treatment for 4 hours during each session, excluding travel (Dhondt et al., 2000). Patients would face difficulty in their job commitments due to constant absence from work during

treatment periods. Patients without a flexible working hour job might lose their source of income once the long-term treatment begins, which would directly cause the country to lose its workforce. They would not only become a liability to the country, but also a long-term financial burden for themselves and to the national healthcare system. In 2013, the total number of end stage renal disease (ESRD) patients in Malaysia amounts to 26,159 and is estimated to increase 4,000 yearly. Statistically, 14 out of 100,000 people suffers from kidney failure (Cheng, 2013).

The dialysis process itself is a long-term painful and expensive process, not only does CKD cause physically difficulty, but also mental stress. Hemodialysis takes a serious toll on patients, as side effects include shortness of breath, nausea and vomiting (Cukor et al., 2013; Vasilopoulou et al., 2015). Patients are also prone to mental side effects as depression since most of them have to make drastic changes in their home or work life and even to the extent of giving up certain responsibilities or activities. Patients no longer have the ability being away from designated dialysis centres, let alone the luxury to travel. Due to its bulky size and imperfect uremic toxin removal, hemodialysis is merely a life support once a patient's kidneys lose their functionality.

In the recent decade, wearable artificial kidney models (based on present hemodialysis design) are developed to solve the shortcomings of hemodialysis. At present, the frontrunner model developed by Gura and co-workers are undergoing clinical trials since early 2010 (Gura et al., 2009; Gura and Rambod, 2010; Davenport, 2015). However, the Gura prototype is still under research and mainly utilises ordinary activated carbon as the adsorbent. These miniaturised models are made possible due to the key component designed in these models, i.e. dialysate regenerative system. The bulk amount of dialysate fluid is regenerated using only

activated carbon as a solid sorbent. Without a deep understanding of biomaterials engineering and adsorbent–adsorbate chemistry, the load/capacity, efficiency and effectiveness of the mentioned prototype is limited and rigid, i.e. degree of miniaturisation is inhibited by the adsorbent design.

1.2 Problem Statement

Firstly, the limitations of the conventional hemodialysis, based on brief literature covered in the previous section (Section 1.1 Research Background), i.e. bulky device which hinders patient mobility, could be overcome by the introduction of wearable artificial kidney models. Table 1.1 shows the comparison between the hemodialysis and an ideal artificial kidney. Hemodialysis based wearable artificial kidney systems are still at clinical trial stages at best. The introduction of nanoporous adsorbent in the form of activated carbon could effectively reduce the amount of dialysate fluid through active and continuous adsorption of uremic toxins from the dialysate fluid.

Table 1.1: Hemodialysis and ideal artificial kidney

Hemodialysis	Ideal artificial kidney
Intermittent	Continuous
Retention of middle molecules Retention of protein bound uremic toxins	Indiscriminate removal of uremic toxins
Bulky	Portable Light weight

Secondly, the materials selection for the choice of adsorbent used for dialysate regeneration has been limited to only activated carbons, as evidently employed in all reviewed patents. The only alternative nanoporous adsorbent studied,

aside from activated carbon (Gura et al., 2009), is zeolite (Wernert et al., 2006; Wernert et al., 2005). These reports indicate that zeolite is better suited for the adsorption of middle molecules such as creatinine and p-cresol. The uremic toxins targeted in this study are urea and uric acid, which belong to the uremic toxin group of small molecules. The study on alternative nanoporous biomaterials which could produce better uremic toxin adsorption results would be highly valuable as the wearable artificial kidney models could be further miniaturised through reduced dialysate amount used in such systems. The amount of adsorbent materials for the dialysate regenerative system could also be reduced, thus a significant reduction in size and weight of the wearable device. The indication on the adsorption performance of a material used in this project is the mass of uremic toxin removed by a fixed amount of adsorbent, expressed in the form of mg/g. A higher number in such case would indicate more uremic toxin removed by the same amount of adsorbent. Apart from scalability size-wise, the duration of use for these higher adsorption nanoporous materials could be extended, i.e. the frequency of change of adsorbent materials (in cartridge form) is prolonged for the same amount of material. This project is focused on the development of improved alternative nanoporous adsorbents, i.e hollow activated carbon fibre, mesoporous silica and mesoporous hydroxyapatite, for the intended application of uremic toxin adsorption for wearable artificial kidney systems. Each of the three nanoporous biomaterials were selected based on the individual improvements in terms of physical properties (surface area) and chemical functionality (surface functional group and biocompatibility).

Hollow activated carbon fibre was selected as an alternative nanoporous adsorbent material due to its higher surface area and shorter diffusion length. The hollow macropore channels enables shorter access of flowing adsorbates into the

micropores of this activated carbon, i.e. better adsorption kinetics (Bandosz, 2006). Access to micropores for conventional powdered or granular activated carbon are more restricted in comparison due to the lack of macropore (only mesopores). Mesoporous silica on the other hand, was selected due to the fact that the flexibility of surface functionalisation (Matsumoto et al., 2006). Active functional groups could be grafted and anchored on the surface of mesoporous silica to selectively target identified functional groups of uremic toxins urea (amine group) and uric acid (carbonyl group). The third nanoporous biomaterial, mesoporous hydroxyapatite, was selected due to its excellent biocompatibility (Akao et al., 1981; Selvakumar et al., 2015) and good protein adsorption (Shen et al., 2008).

1.3 Research Objectives

The purpose of this research is to explore potential alternative biomaterials for uremic toxin adsorption. Material selection for this application is limited to activated carbon as the sole adsorbent on this list. Research objectives for this project are:

1. To synthesise and characterise three nanoporous biomaterials, i.e. activated carbon fibre, mesoporous silica and mesopores hydroxyapatite for urea and uric acid adsorption.
2. To evaluate the urea adsorption capacity of activated carbon fibre, mesoporous silica and mesopores hydroxyapatite.
3. To study the kinetics and mechanisms of urea and uric acid adsorption by activated carbon fibre, mesoporous silica and mesopores hydroxyapatite.